

COB-2023-1752

ANALYSIS OF ENRICHMENT FUNCTIONS IN FEM FOR SIMULATING CRACKED SHEET METAL

Gustavo Alves Lima

Instituto Federal do Espírito Santo (IFES) – Campus São Mateus, São Mateus-ES, Brasil, CEP: 29932-540.
2001gustavoalves@gmail.com

Carlos Roberto Barcellos

Instituto Federal do Espírito Santo (IFES) – Campus Vitória, Vitória-ES, Brasil, CEP: 29040-780.
barcello@gmail.com

Werley Gomes Facco

Instituto Federal do Espírito Santo (IFES) – Campus São Mateus, São Mateus-ES, Brasil, CEP: 29932-540.
werleyfacco@gmail.com

Abstract. *In most engineering problems modeled by differential equations, obtaining an analytical solution is unfeasible or even impossible, which makes numerical approaches essential in this analysis. In the field of Solid Mechanics, the Finite Element Method (FEM) is a robust, versatile and consolidated numerical technique, but it still has limitations. The enrichment of the function space of the FEM can reduce some limitations of the method as it inserts a priori information about the expected result of the problem, contributing to increase the space of interpolation functions of the method and reducing the impact of the mesh in the simulation. In this context, this research aims to select and apply enrichment functions in the FEM, inserted locally on the contours of the hole in a surface loaded. The results obtained with the enriched FEM are compared with the traditional FEM. As enrichment functions, polynomial functions and trigonometric functions derived from Fracture Mechanics analysis for some crack models are applied. It was observed that the application of the enrichment functions reduced the simulation error for the same finite element mesh, and the functions that models triples can be used as an alternative to 1st polynomials.*

Keywords: *Finite Element Method, Fracture Mechanics, Generalized Finite Element Method.*

1. INTRODUCTION

In most engineering problems modeled by differential equations, obtaining an analytical solution is unfeasible or even impossible, which makes numerical approaches essential for the analysis of these phenomena (Polycarpou, 2008). In the field of Solid Mechanics, the Finite Element Method (FEM) is a robust, versatile and consolidated numerical technique (Kim and Sankar, 2012). However, its application still has limitations. Reducing the limitations of the FEM allows more accurate simulations to be performed with computationally less expensive algorithms.

In Fracture Mechanics, two characteristics of FEM make the numerical analysis of crack propagation in materials difficult: one refers to the adequate choice of mesh, which must be more refined in regions where the solution presents higher gradients; moreover, in problems whose domain varies with time, the creation of meshes every instant to follow changes in the domain increases the computational cost of the approach (Polycarpou, 2008; Liu and Gu, 2005). The enrichment of the function space of the FEM can reduce these and other limitations of the method as it inserts a priori information about the expected result of the problem, contributing to increase the space of interpolation functions of the method and reducing the impact of the mesh in the simulation (Facco, 2012).

The enrichment of FEM basis functions by polynomials is a common option, mainly due to the ease of implementation and the ability to satisfactorily approximate smooth functions (Paiva, 2017). On the other hand, it is expected that functions that analytically describe the stress behavior of cracked plates can be an alternative to polynomials, since they are functions closer to the expected result of the simulation.

Therefore, this work analyzes the use of enrichment functions in the Finite Element Method when applied to problems of linear elastic deformation in a plane stress state, whose domain presents a crack. As enrichment functions, the use of 1st and 2nd degree polynomials was evaluated; of functions that model elliptical triplets; and a combination of these. The plane deformation problem presented in (Szabo and Babuska, 1935) was evaluated, whose analytical solution can be estimated. The performance of numerical methods in the calculation of nodal displacements was evaluated, since it is the variable directly calculated by the method.

2. EQUATION OF THE PROBLEM

In plane stress problems, the domain of interest has a very small length (measured in the z direction) compared to the other two dimensions (x and y directions), and the stress component acting in the z direction is zero (Liu and Gu, 2005). Thus, consider a plate in a plane stress state, with the Ω domain delimited by a surface Γ , so that $\Gamma = \Gamma_t \cup \Gamma_u$ and $\Gamma_t \cap \Gamma_u = \emptyset$, show in Figure 1.

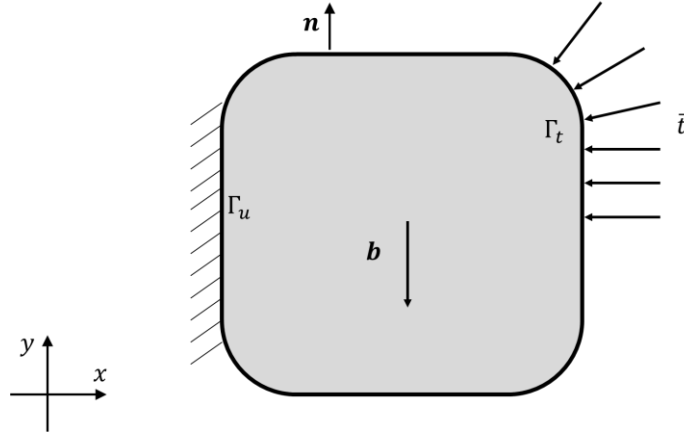


Figure 1. Continuous solid Ω and applicable loading conditions.

According to Liu and Gu (2005), the differential equation that models deformation problems in a plane stress state is given by the equation

$$\mathbf{L}\boldsymbol{\sigma} + \mathbf{b} = \mathbf{0}, \quad (1)$$

where \mathbf{b} is the body force (referring to a force that acts over the entire extension of the domain, such as gravitational force, neglected in this work) and $\boldsymbol{\sigma}$ is a stress tensor, defined as

$$\boldsymbol{\sigma} = \begin{Bmatrix} \sigma_x \\ \sigma_y \\ \tau_{xy} \end{Bmatrix}. \quad (2)$$

The stress tensor can be associated with deformation and nodal displacements by constitutive relations (Liu and Gu, 2005), and can be written as

$$\boldsymbol{\sigma} = \mathbf{D}\mathbf{L}^T \mathbf{u}, \quad (3)$$

where \mathbf{L} is a differential operator (Eq. (4)), \mathbf{D} is a characteristic matrix of the material (Eq. (5), for linear isotropic materials, where E and ν are, respectively, the modulus of elasticity and the Poisson coefficient of the material) and \mathbf{u} is the displacement of the body points, presenting the components $\mathbf{u} = \{u_x, u_y\}^T$ in the Cartesian orientation system.

$$\mathbf{L} = \begin{bmatrix} \frac{\partial}{\partial x} & 0 \\ 0 & \frac{\partial}{\partial y} \\ \frac{\partial}{\partial y} & \frac{\partial}{\partial x} \end{bmatrix}. \quad (4)$$

$$\mathbf{D} = \frac{E}{1-\nu^2} \begin{bmatrix} 1 & \nu & 0 \\ \nu & 1 & 0 \\ 0 & 0 & \frac{1-\nu}{2} \end{bmatrix}. \quad (5)$$

The boundary conditions are:

$$\mathbf{u} = \bar{\mathbf{u}}, \quad \forall (x, y) \in \Gamma_u \quad (6)$$

and

$$\boldsymbol{\sigma} \mathbf{n} = \bar{\mathbf{t}}, \quad \forall (x, y) \in \Gamma_t, \quad (7)$$

where $\mathbf{n} = \{nx, ny\}^T$ is the normal vector, $\bar{\mathbf{u}}$ are the known displacement and $\bar{\mathbf{t}}$ is the applied stress.

Applying the weighted residuals method or energy methods on the governing equation, one can find the Weak Form of the problem (Eq. (8)), where $\boldsymbol{\phi} = \{\phi_x, \phi_y\}^T$ is the test function and $\mathbf{T} = \{T_x, T_y\}^T$ is the tension applied on Γ (Chandrupatla and Belengundu, 2010).

$$\int_{\Omega} \left(\sigma_x \frac{\partial \phi_x}{\partial x} + \tau_{xy} \frac{\partial \phi_x}{\partial y} + \tau_{xy} \frac{\partial \phi_y}{\partial x} + \sigma_y \frac{\partial \phi_y}{\partial y} \right) dA = \int_{\Gamma} (T_x \phi_x + T_y \phi_y) d\Gamma, \quad (8)$$

In the FEM, the function \mathbf{u} is approximated by interpolating the base functions according to Eq. (9), where n is the number of mesh nodes that discretize the domain and N_i is the i -th shape function. In this work, 1st degree polynomial basis functions were used, as per (Kim and Sankar, 2002; Chandrupatla and Belengundu, 2010; Polycarpou, 2008).

$$\mathbf{u} \cong \mathbf{u}^T = \sum_{i=1}^n u_i \cdot \mathbf{N}_i. \quad (9)$$

In the enrichment of the FEM, the enrichment functions $\boldsymbol{\psi}_{ij}$ are inserted, so that the solution is approximated by (Silva, 2015)

$$\mathbf{u}^T = \sum_{i=1}^n (u_i \cdot \mathbf{N}_i + \sum_{j=1}^q (b_j \cdot \mathbf{N}_i \cdot \boldsymbol{\psi}_{ij})), \quad (10)$$

where q is the number of enrichment functions associated with node i .

The algorithms used in this work were implemented in the MATLAB software version R2022B in an Intel Pentium Gold 7505 notebook, with 4Gb of RAM and Windows 10 Operating System, using the Bella10 to build the meshes. The integrals calculated in the FEM were performed by Gaussian quadrature. Material parameters were defined as $E = 1000\text{Pa}$ and $\nu = 0.3$, as presented in Szabo and Babuska (1935), and a tension of 1 Pa was used.

3. SELECTION OF THE ENRICHMENT FUNCTION IN FRACTURE MECHANICS

In Anderson (2008), there is a description of analytical models that describe the behavior of stress and displacements around cracks in bodies stressed by different modes of loading. The nodal displacements generated at the tip of a crack (Figure 2) are described by the equations in Table 1, in which the loading modes I and II correspond to the opening and shear loading in the plane crack, respectively.

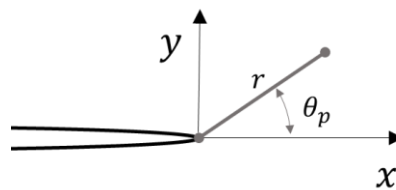


Figure 2. Definition of the Cartesian (pair (x, y)) and polar (pair (r, θ_p)) coordinate axes at the crack tip.

Table 1. Displacement field at the tip of a crack in loading modes I and II, in Linear Elastic and Isotropic material.

	Loading Mode I	Loading Mode II
u_x	$\frac{K_I}{2\mu} \sqrt{\frac{r}{2\pi}} \cos\left(\frac{\theta_p}{2}\right) \left[\kappa - 1 + 2 \sin^2\left(\frac{\theta_p}{2}\right) \right]$	$\frac{K_{II}}{2\mu} \sqrt{\frac{r}{2\pi}} \sin\left(\frac{\theta_p}{2}\right) \left[\kappa + 1 + 2 \cos^2\left(\frac{\theta_p}{2}\right) \right]$
u_y	$\frac{K_I}{2\mu} \sqrt{\frac{r}{2\pi}} \sin\left(\frac{\theta_p}{2}\right) \left[\kappa + 1 - 2 \cos^2\left(\frac{\theta_p}{2}\right) \right]$	$-\frac{K_{II}}{2\mu} \sqrt{\frac{r}{2\pi}} \cos\left(\frac{\theta_p}{2}\right) \left[\kappa - 1 - 2 \sin^2\left(\frac{\theta_p}{2}\right) \right]$

μ is the shear modulus, $\kappa = (3 - \nu)/(1 + \nu)$ for plane state problems of voltages and K_I and K_{II} are characteristic values of the problem.

Thus, the following functions will be used as an enrichment function:

$$MF_1 = \sqrt{r} \cdot \sin\left(\frac{\theta_p}{2}\right), \quad (11)$$

$$MF_2 = \sqrt{r} \cdot \cos\left(\frac{\theta_p}{2}\right), \quad (12)$$

$$MF_3 = \sqrt{r} \cdot \sin^2\left(\frac{\theta_p}{2}\right) \cdot \cos\left(\frac{\theta_p}{2}\right), \quad (13)$$

$$MF_4 = \sqrt{r} \cdot \sin\left(\frac{\theta_p}{2}\right) \cdot \cos^2\left(\frac{\theta_p}{2}\right), \quad (14)$$

and

$$MF_5 = \sqrt{r} \cdot \sin\left(\frac{\theta_p}{2}\right) \cdot \cos\left(\frac{\theta_p}{2}\right). \quad (15)$$

Note that functions MF_1 , MF_2 , MF_3 and MF_4 are the basis of the equations in Table 1, and function MF_5 complements the composition of sines and cosines. The creation and use of MF_5 allows the grouping of five functions derived from Fracture Mechanics (named MF Functions) for a better comparison with 2nd degree polynomials, which have five monomials. Similar functions were used in (Legrain et al., 2005; Silva, 2015) with good results.

4. RESULTS AND DISCUSSIONS

The analysis of the problem was carried out in three stages. In the first stage, the numerical model was validated based on the problem proposed by Szabo and Babuska (1997). The problem consists of an infinite plate pulled by a load σ_x with a circular hole of radius a . To simulate the problem, the domain was truncated, limiting it to a square of side $2b$, which is reduced to a square of side b by applying symmetry conditions, as shown in Figure 3. In this work, $a = 1$ was adopted.

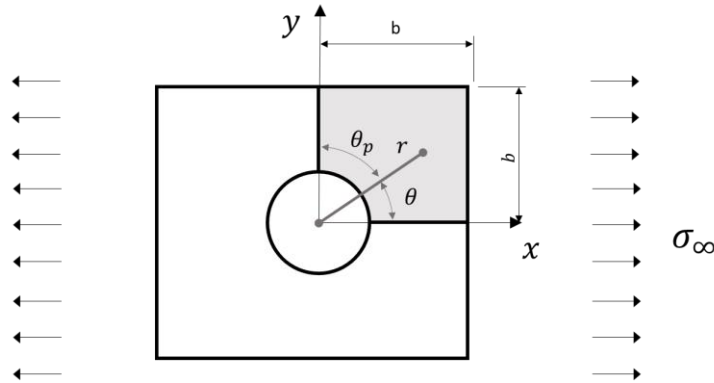


Figure 3. Domain of the problem analyzed and guidance system used.

The solution to the problem is given in Eq. (16) and (17), valid for $b \rightarrow \infty$.

$$u_x = \frac{\sigma_\infty a}{8G} \left[\frac{r}{a} (\kappa + 1) \cos \theta + 2 \frac{a}{r} ((1 + \kappa) \cos \theta + \cos 3\theta) - 2 \frac{a^3}{r^3} \cos 3\theta \right]. \quad (16)$$

$$u_y = \frac{\sigma_\infty a}{8G} \left[\frac{r}{a} (\kappa - 3) \sin \theta + 2 \frac{a}{r} ((1 - \kappa) \sin \theta + \sin 3\theta) - 2 \frac{a^3}{r^3} \sin 3\theta \right]. \quad (17)$$

To evaluate the minimum size of the square in which the solution of Eq. (16) and (17) was still valid, b was varied from 3 to 24 and the simulation error was calculated by applying the traditional FEM with a very fine mesh (with elements of characteristic length $h = 0.1$), selecting the ideal size b so that the error in the simulation was below 10^{-2} , a value similar to that found in (Barcellos et al., 2022). Afterwards, the convergence of the method was evaluated by analyzing the variation of the error with the refinement of the mesh in order to affirm the choice of the initial parameter $h = 0.1$ and to show that the modeling via FEM was coherent.

The calculated error was the relative error in the L2 norm, according to (Facco, 2012), applied in the calculation of the nodal displacements in the two Cartesian directions, being evaluated globally and locally on a 3x3 square around the discontinuity.

Figure 4 and 5 shows the local and global error variation with increasing size of the computational domain side, applying the traditional FEM.

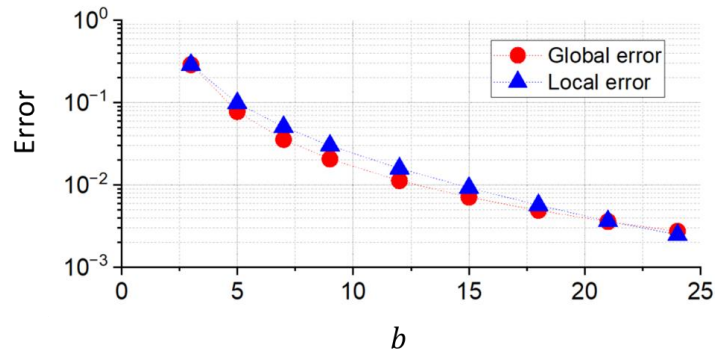


Figure 4. Variation of the error in the calculation of displacements in x direction by the FEM with the increase in the domain length (b) for a very refined mesh.

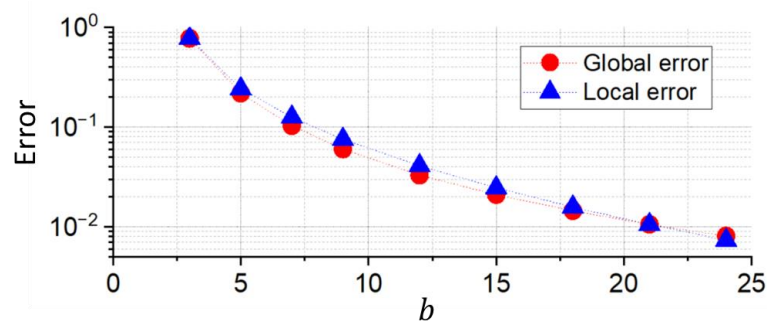


Figure 5. Variation of the error in the calculation of displacements in y direction by the FEM with the increase in the domain length (b) for a very refined mesh.

Note that all errors are below 10^{-2} from the grid with 24 units on a side. Thus, this size was used for the analysis of the enrichment functions.

Applying the traditional FEM, the error reduction according to the mesh refinement using $b = 24$ is observed in Figures 6 and 7, where \sqrt{n} is the square root of the number of mesh nodes. Note that the global error is always below the 10^{-2} tolerance, and that the local error becomes acceptable in meshes from 150^2 nodes. In the mesh with approximately 150^2 nodes, the mesh parameter is $h = 0.158$.

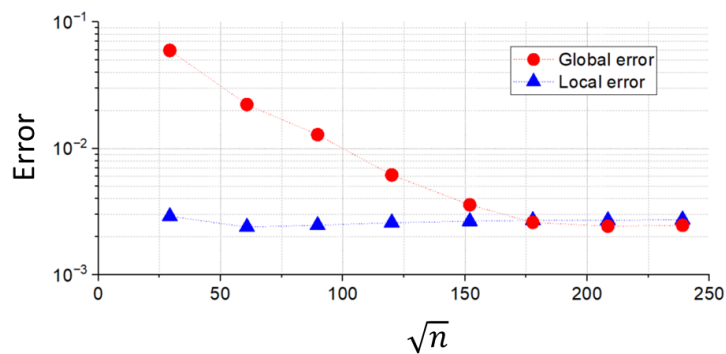


Figure 6. Variation of the local and global error in the x Direction displacements by FEM according to mesh refinement.

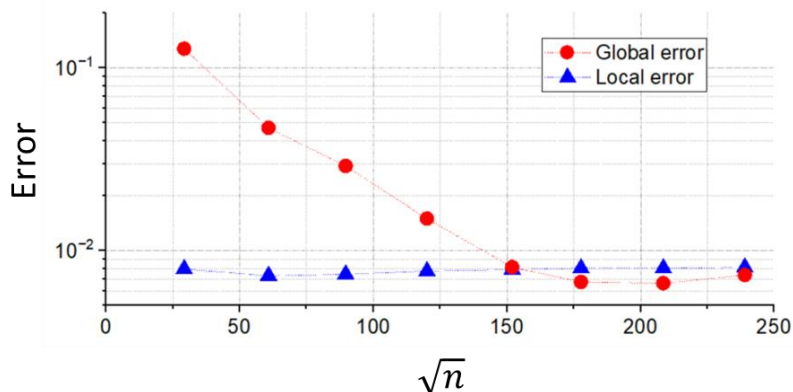


Figure 7. Variation of the local and global error in the y Direction displacements by FEM according to mesh refinement.

In the second stage, the performance of the enrichment functions in the FEM was evaluated, analyzing only the local error of the simulation, since the global effects of the discontinuity are not very significant, as shown in Figure 6 and 7. Only the nodes in the contour of the hole are enriched. Three groups of enrichment functions were used:

- 1st degree monomials: $\{x, y\}$
- 2st degree monomials: $\{x, y, xy, x^2, y^2\}$
- Functions based on Fracture Mechanics: MF_1, MF_2, MF_3, MF_4 e MF_5 .

From the results of the first stage, the mesh parameter is found in which the FEM solves the problem within the established tolerance ($h = 0.158$). Thus, the mesh refinement was varied locally (h varying from 0.15 to 0.50 in a 3×3 square close to the discontinuity, keeping the characteristic length 0.158 in the rest of the domain), calculating the corresponding error.

Figure 8 and 9 show the error reduction with local mesh refinement using 1st and 2nd degree polynomials and with the MF Functions. Note that all enrichments performed better than the traditional FEM, generating less error for the same finite element mesh. The use of MF Functions showed a greater error reduction than the use of 1st degree Polynomials, but worse than the 2nd degree Polynomials. Thus, it is not advantageous to use the five MF functions together: they present a computational cost similar to that of 2nd degree polynomials, but with inferior performance.

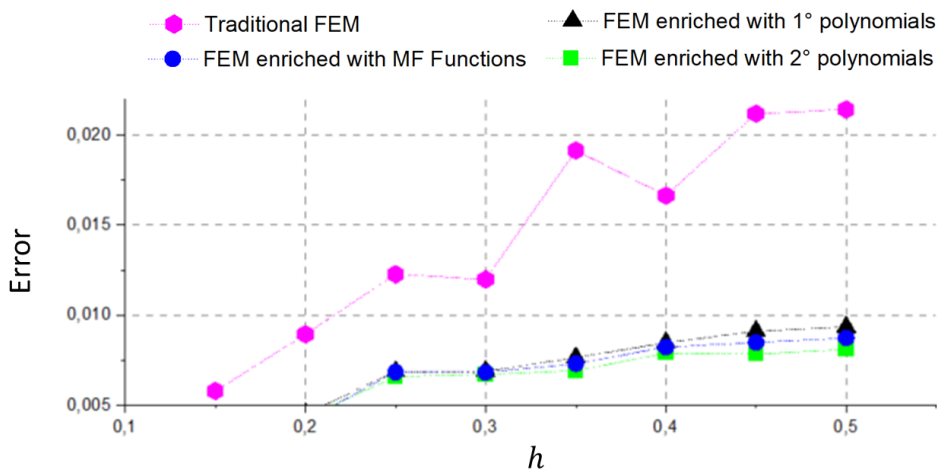


Figure 8. Variation of the error in the calculation of displacements in the x direction near the discontinuity with the local refinement of the mesh with the MEF and the enrichment proposals.

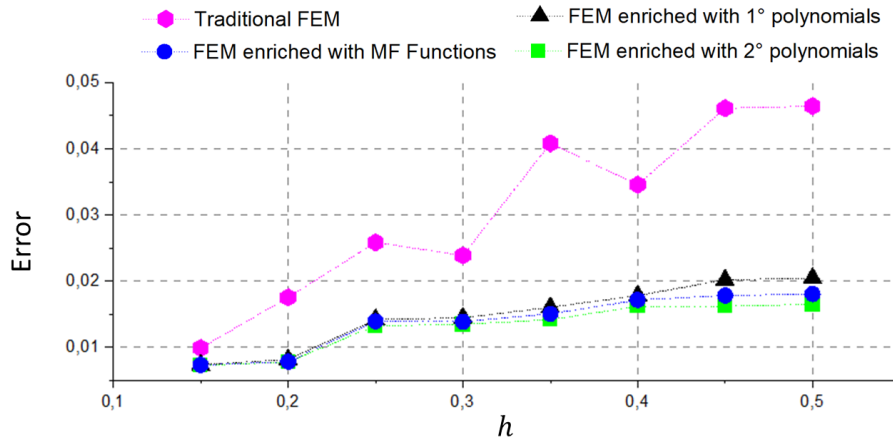


Figure 9. Variation of the error in the calculation of displacements in the y direction near the discontinuity with the local refinement of the mesh with the MEF and the enrichment proposals.

In the third step, the performance of all enrichment functions was evaluated separately. Based on this result, two combinations of functions were analyzed:

- Combination 1: five functions that performed best.
- Combination 2: two of the best performing Fracture Mechanics functions.

Based on numerical experiments, the following combinations were chosen:

- Combination 1: y , x^2 , MF_1 , MF_2 and MF_5 .
- Combination 2: MF_1 and MF_2 .

The results obtained with these functions are shown in Figure 10 and 11. Note that Combination 2 presented a behavior similar to the use of 1st degree Polynomials and Combination 1 presented the same tendency of behavior as the use of the five functions of the Mechanics of Fracture analyzed together.

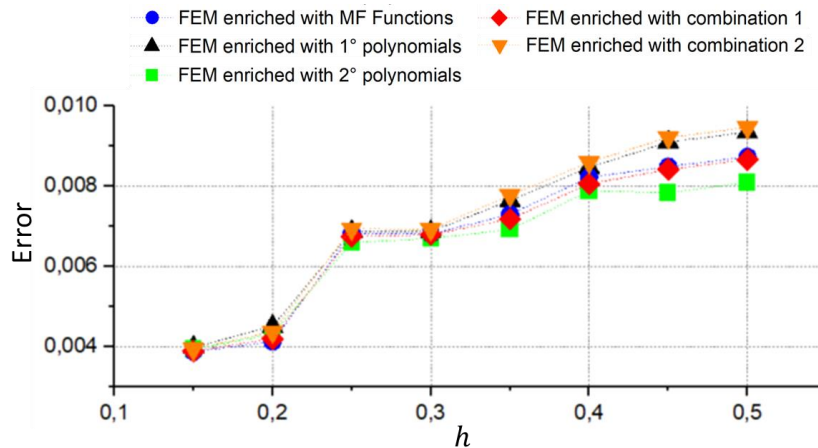


Figure 10. Error variation in the calculation of displacements in the x direction according to local mesh refinement, comparing the initial proposals with the combinations.

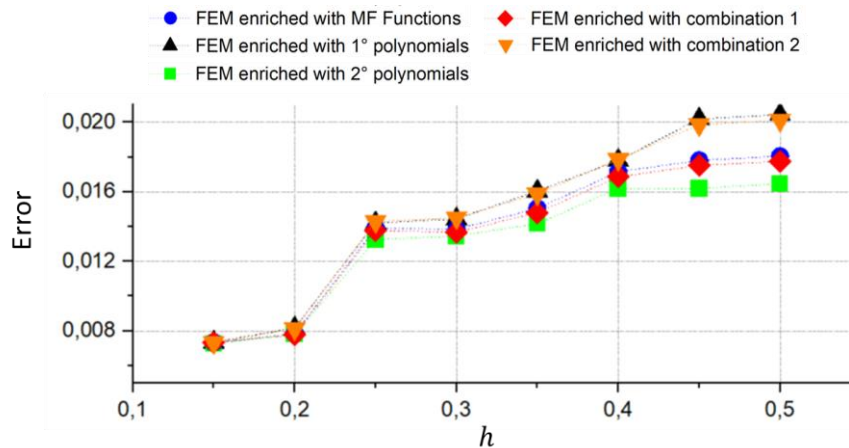


Figure 11. Error variation in the calculation of displacements in the y direction according to local mesh refinement, comparing the initial proposals with the combinations.

In this way, the use of Combination 2 can be an alternative to the use of 1st degree polynomials. However, the MF functions were not able to compete with polynomials of higher degree because the use of polynomials generated less error for the same mesh and due to the difficulty of integration (since polynomials are analytically integrated in triangular elements in the FEM).

5. CONCLUSION

In this work, the enrichment in the FEM by polynomials and by trigonometric functions based on analytical models from Fracture Mechanics was compared in a deformation problem in sheet metal with a circular hole. All enrichment proposals were satisfactory, since it reduced the error in the calculation of plate displacements for the same finite element mesh, reducing the impact of the mesh in the simulation. The results showed that using as enrichment functions the Fracture Mechanics functions that model cracks can be an alternative to the use of 1st degree polynomials. However, it was uncompetitive with the use of higher degree polynomials, because in addition to the greater error reduction, there is the guarantee of analytical integration when using polynomials.

6. ACKNOWLEDGEMENTS

This work was partially supported by the FAPES, FAPEMIG, CNPq and CAPES.

7. REFERENCES

- Anderson, T. L., 2017. *Fracture mechanics: fundamentals and applications*. CRC press.
- Chandrupatla T. R. and Belegundu A. D., 2014. *Finite Element (in Portuguese)*. 4^a. Ed. Person.
- Facco, W. G., 2012. *Treatment of Material Discontinuity in the Generalized Finite Element Method (in Portuguese)*. Ph.D. thesis, Graduate Program in Electrical Engineering, Federal University of Minas Gerais, Belo Horizonte, Brasil.
- Kim, N. and Sankar, B. V., 2012. "Introduction to Finite Element Analysis and Design".
- Legrain, G., Moes, N. and Verron, E., 2005. Stress analysis around crack tips in finite strain problems using the eXtended finite element method. *International Journal for Numerical Methods in Engineering*, 63 (2), pp.290 - 314.
- Liu, G.R. and Gu Y. T., 2005. "An Introduction to Meshfree Methods and Their programming", Singapore, Springer.
- Paiva, G.O. F., 2017. *Application and Analysis of MEF with Polynomial Enrichment in the Simulation of Structures in the Process of Damage (in Portuguese)*. Master's thesis, Department of Civil and Environmental Engineering, University of Brasilia, Brasilia/DF, Brasil.
- Polycarpou, A.C. 2006. "Introduction to Finite Element Method in Electromagnetics", United States of America, First Edition.
- Silva, P. A. B. V., 2015. *An implementation of the Extended Finite Element Method for Two-dimensional Fracture Propagation Analysis (in Portuguese)*. Master's thesis, Department of Civil Engineering of the Center Scientific Technician at PUC-Rio, Pontificia Catholic University of Rio de Janeiro, Rio de Janeiro, Brasil.
- Szabo, B. and Babuska, I., 1935. "Finite Element Analysis". John Wiley & Sons, United States of America.

8. RESPONSIBILITY NOTICE

The authors are the only responsible for the printed material included in this paper.